



ANSYS MODELING OF POST-TENSIONED STEEL BEAM-COLUMN CONNECTIONS UNDER CYCLIC LOADING

Saber Moradi

Ph.D. Candidate, the University of British Columbia, Canada

M. Shahria Alam

Associate Professor, the University of British Columbia, Canada

ABSTRACT

Permanent deformations in a steel moment resisting frame can be eliminated by using post-tensioned (PT) elements. This paper presents the development of three-dimensional finite element models of PT steel beam-column connection subassemblies. Knowing that there is limited experimental data in the literature on PT steel connections with top-and-seat angles, reliable finite element models can be used to investigate the load carrying behaviour of PT steel connections as well as producing more data for these new connections. In this paper, finite element modelling, meshing, and analysis are performed in the commercial software, ANSYS. The analysis includes geometric and material nonlinearities, pre-loaded bolts and strands, gap opening and closing behaviour, in addition to contact and sliding phenomena. The results of finite element simulations are verified against previous test results on five interior PT steel beam-column connections with top-and-seat angles. In addition, parametric studies are conducted to investigate the effects of three factors on the cyclic response of PT steel connections. These factors include the yield strength and strain hardening of steel angles, the amount of initial post-tension force in PT strands, and the use of beam flange reinforcing plates.

Keywords: Steel Connections, Beam-Column Connections, Post-Tensioned, Self-Centering Steel Frames, Cyclic Loading, ANSYS simulation.

1. INTRODUCTION

Since the 1994 Northridge earthquake, several efforts have been made to improve the seismic design and resistance of steel buildings. Nonetheless, permanent damage may still occur in steel framed buildings under moderate and strong excitations; this permanent structural damage is expected because the design of these steel buildings is based on the ductility of steel material. To eliminate permanent deformations in steel buildings, various new techniques have been proposed and investigated by researchers. Several studies have examined the applications of smart materials, such as Shape Memory Alloys (SMAs) in civil engineering structures (Menna et al. 2015); SMA-based bracing systems (e.g., Moradi et al. 2014), beam-column connections (e.g., Moradi & Alam 2015), as well as isolation and retrofitting devices (e.g., Ozbulut et al., 2011) are a few examples of such applications. However, the practical applications of SMAs are currently hindered by several factors, including cost, manufacturing, material training, and lack of reliable joining techniques.

Another alternative is to allocate pre-specified elements in a building so that damage is confined to easily repairable/replaceable components. Thus, the main structural elements remain elastic and consequently, residual deformations can be eliminated after replacing the damaged elements. Many researchers have studied self-centering systems (Hajjar et al. 2013) for building applications. Among these systems, the application of post-tensioned (PT) strands or bars in buildings and bridges have attracted much interest in recent years. Ricles et al. (2001) was the first study that extended the use of PT elements to steel moment connections. In a PT steel frame, beams are pre-compressed to columns using PT steel bars or strands, which run parallel to beams and pass through column flanges. The main purpose of using the PT elements anchored at exterior columns is to provide self-centering in the building. The flag-shape response of a PT beam-column connection, is governed by gap-opening and closing behaviour at the

connection interface. In frames with PT connections, supplemental energy dissipation is provided through yielding or friction devices. PT connections with steel angles (Ricles et al. 2002; Garlock et al. 2005), friction devices (Wolski et al. 2009; Rojas et al. 2005), buckling-restrained bars (Christopoulos et al. 2002), and web hourglass-shaped pins (Vasdravellis et al. 2013b) are among many other studies on PT steel connections and frames. A recent overview of PT steel connections is available in Moradi & Alam (2016).

The self-centering response is achieved in a PT steel frame as long as brittle failure and damage states, such as beam local buckling and PT strand fracture are prevented through a comprehensive design (Garlock et al. 2007; Kim & Christopoulos 2009b). In the absence of adequate experimental studies, finite element analyses can be used to investigate the complex behaviour of these connections (Kim & Christopoulos 2009a; Moradi et al. 2015; Vasdravellis et al. 2013a). In this paper, three-dimensional finite element modeling of large-scale PT steel beam-column connection subassemblies with bolted angles is described. A detailed study is presented describing the options that were found useful in avoiding convergence problems in the nonlinear finite element modeling of PT connections. The modeling techniques can be also useful for simulation of other types of steel connections.

2. DETAILS OF PT BEAM-COLUMN CONNECTION SPECIMENS

The experiment on interior PT connections performed by Ricles et al. (2002) was used as a basis for verifying the accuracy of the finite element simulations. Figure 1 shows a schematic view of these connections with PT strands and top-and-seat angles. The connections have W24×62 wide flange beams and a W14×311 wide flange column. Other components in the tested connection specimens are angles, bolts, bearing plates, PT strands, shim plates and beam flange reinforcing plates. From the connections tested in Ricles et al. (2002), five specimens were modeled in ANSYS (Release 15, 2013). Table 1 summarizes the angle sizes and gage-length to-thickness (g/t) ratios for the steel angles in each specimen. The gage length, g, is the distance between the fillet of the angle leg (attached to the column) and the edge of the bearing plate. The connections have four high-strength post-tensioning strands on each side of the beam running parallel to the beam. Table 1 also lists the ratio between the initial post-tensioning force in a PT strand, T_i , and its ultimate tensile strength ($T_u = 261$ kN).

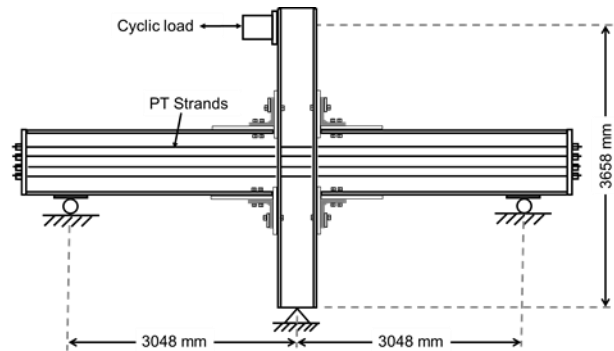


Figure 1: Schematic of a PT connection modeled in this study (adapted from Ricles et al. 2002; Moradi & Alam 2016)

Table 1: PT connections modeled as per the experiment in Ricles et al. (2002).

| PT connection | Angle size | t (mm) | g/t | T_i/T_u |
|---------------|---------------|--------|-----|-----------|
| PC1 | L152×152×7.9 | 7.9 | 9.0 | 0.36 |
| PC2 | L152×152×7.9 | 7.9 | 4.0 | 0.37 |
| PC3 | L203×203×15.9 | 15.9 | 7.2 | 0.34 |
| PC4 | L203×203×15.9 | 15.9 | 4.0 | 0.34 |
| PC5 | L203×203×25.4 | 25.4 | 4.0 | 0.34 |

3. FINITE ELEMENT MODELS

All the simulations in this study were performed using the Mechanical APDL tools in the finite element Software, ANSYS. Figure 2 shows the three-dimensional solid model for PT Connection specimen PC4. Since dealing with a large model is expensive in terms of computational time and resources, a few assumptions were made to alleviate this matter. Considering a symmetry condition, half of the beam-column connection was modeled. In addition, welding was not explicitly modeled. The welded components were modeled by constraining all degrees-of-freedom for appropriate volumes (for example, the beam flange and the beam reinforcing plate). The main challenge in such finite element simulations is to overcome convergence difficulties, especially when the finite element analysis involves a nonlinear problem with sliding and contact behaviour. In the next sections, we discuss the techniques that were found helpful in avoiding divergence in the finite element analysis.

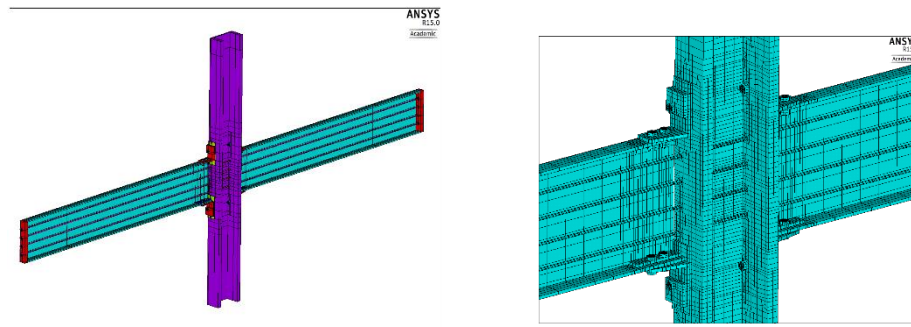


Figure 2: Specimen PC4: volume and meshing details

To improve the accuracy of the simulation, solid models were developed for all the components (including the bolts). By modeling 75% of the area corresponding to the nominal bolt diameter, the reduction of the cross-sectional area of the bolt shank, due to the threads, was included in the models (Kulak 2005). The generation and analysis of the finite element models involve defining material properties, meshing, assigning boundary conditions, loading and analysis. These tasks are demonstrated in the following sections.

3.1 Material properties

A bilinear elasto-plastic behaviour was assigned for the material property of steel in all the components, except for the bolts (see Figure 3). For the modeling of high strength bolts, the trilinear relationship in Figure 3(b) was defined. The strain hardening (α) was assumed to be 0.05, and 0.02 for steel in PT strands and angles, respectively, while the strain hardening for other components was taken as 0.01. The modulus of elasticity, E and Poisson ratio for steel material were assumed to be 200 GPa and 0.3, respectively. Material yielding was set to be predicted using *von Mises* yield criterion, as well as the Kinematic strain hardening and the associated flow rule for material post-yield behaviour; the Bauschinger effect is therefore considered in material models. Further details for the material properties can be found in the reference experimental study by Ricles et al. (2002).

3.2 Meshing

The created models were meshed using three-dimensional, 8-node homogeneous solid elements (SOLID185) from the element library available in ANSYS. A mapped mesh with a typical regular pattern was generated for the models. Meshing details for the model of specimen PC4 are shown in Figure 2. Adequately dense meshes should be created in the regions that the behaviour of material and/or components is of interest (such as the connection interface and plastic hinge regions). Fine meshes were also generated for the top-and-seat angles, which are expected to undergo extensive yielding. The convergence of a finite element analysis can be improved by producing consistent and sufficiently dense meshes over contact surfaces. However, finite element analysis of models with finer meshes (greater number of elements) is computationally more demanding. The finite element model for PC4, for instance, consists of 4,212 key points, 10,300 lines, 8,236 areas, 2,150 volumes, 70,022 nodes, and 50,840 elements. To reduce computational time, half of a PT connection was modeled (see Figure 2).

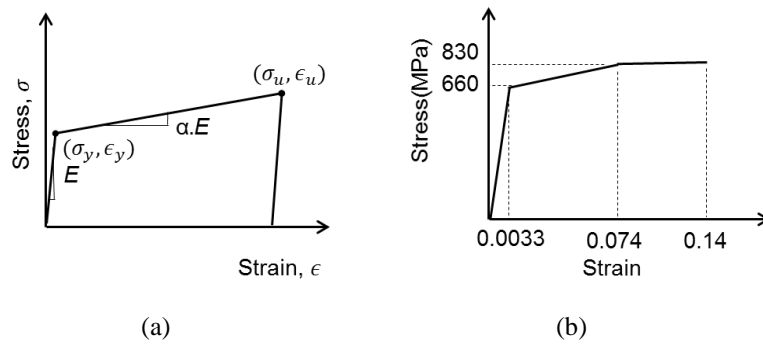


Figure 3: Material properties assumed for: (a) steel and (b) the bolts [adapted from Moradi & Alam (2016)]

3.3 Contact

The interaction between structural components that are in contact may have significant effects on the accuracy of a nonlinear finite element analysis. Here, we used three-dimensional 4-node surface-to-surface contact elements (CONTA173) to model the contact and frictional sliding of the components. By defining contact elements, a deformable surface is created on the solid model; the contact elements are then paired with defined target elements (TARGE170). A contact between two surfaces is initiated when a contact element penetrates into one of the target elements. For all the contact elements, coefficient of friction was set to 0.4. Contact elements were defined between the following structural components: (a) angle leg and the shim plate (or the column in model PC1, which does not have any shim plate); (b) angle leg and the beam flange; (c) beam web/flanges and the shim plate (or the column in model PC1); (d) PT bars and holes in the column flanges. In ANSYS, different key options are available to control element properties, formulations, and outputs. The following key options in ANSYS were used to control element properties, formulations, and outputs for the contact elements:

1. The location of contact detection point was chosen to be on Gauss point. This option generally provides more accurate results.
2. Penalty function was chosen for the contact algorithm.
3. In the analysis, both the initial geometrical penetration (gap) and offset were excluded.
4. The solving program was allowed in the analysis to automatically update contact stiffness values in each iteration (based on current mean stress of underlying elements).

Additionally, two other settings were used in case of convergence difficulties, which were particularly due to the contact between the PT bars and holes on the column flanges. One technique was to assign a lower value than 1 (the default) for normal penalty stiffness factor (FKN) for the contact element. Making a refinement to the allowable stiffness range using the key options for the contact element was the other way to overcome the convergence difficulties associated with the contact phenomena.

3.4 Boundary conditions and loading

Since half of a PT connection was modeled, symmetry conditions (zero out-of-plane displacement) were established for the vertical plane. Pin support conditions were also created for the column base by restraining the vertical and horizontal displacement of the nodes on the centerline. As per the test in Ricles et al. (2002), roller supports were established for the beams.

The horizontal loading was applied to the column flange (nodes at a distance of 3,658 mm from the bottom). According to the experimental test (Ricles et al. 2002), the loading involves cyclic story drifts with amplitudes of 0.1, 0.2, 0.3, 0.4, 0.5, 0.7, 1, 1.5, 2, 2.5, and 3%. Story drift here is defined as the displacement applied on the column flange divided by 3,658 mm. Specimens PC3 and PC4 were loaded up to 3.5% story drifts. In the finite element analysis, the loading was therefore applied as successive cycles of displacement loading on the column.

3.5 Analysis

Before loading the column, pretension forces were created in the bolts and PT strands. This step was carried out using PSMESH and SLOAD commands in ANSYS. The amount of pretension force in the bolts was given equal to 230 kN (RCSC 2009). Afterwards, the displacement drift cycles were applied to the column through several load steps.

A nonlinear static analysis was performed to simulate the cyclic performance of the PT connections. In the analysis, geometric nonlinearity was considered by enabling large deformation effects. The optimized nonlinear solution defaults with automatic time stepping were also enabled. To improve the convergence of analysis, it is important to apply the load very slowly (with small load increments). Additionally, changing the Newton-Raphson options from AUTO (program chosen) to UNSYM (i.e., full Newton-Raphson with unsymmetric matrices of elements where the unsymmetric option exists) is useful to avoid convergence difficulties (ANSYS 2013a). On average, the finite element analysis running time for one model was 7 hour long, using a 64-bit operating system in Win. 7 with an Intel Core i5-3570 CPU at 3.40 GHz and with 8 GB of RAM.

4. VALIDATION OF THE SIMULATIONS

A detailed validation study of the finite element analysis can be found in Moradi & Alam (2016). However, in this section, a summary is presented. Figure 4 depicts the lateral load-displacement response of four specimen (PC1, PC2, PC3, and PC4) along with the corresponding experimental response (Ricles et al. 2002). As seen, very good correlations exist between the analytical and test results.

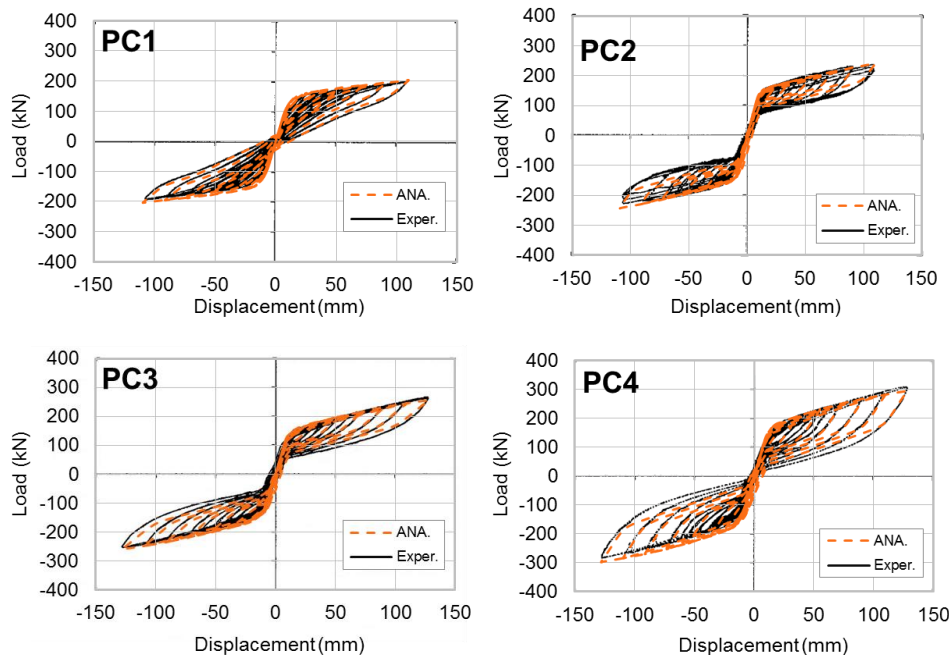


Figure 4: Analytical [Moradi & Alam (2015)] versus experimental response [Ricles et al. (2002)] for specimens PC1, PC2, PC3, and PC4

The finite element analysis shows smaller residual stiffness, a smaller strength, and lower energy dissipation for PC2, which has smaller angles, as was also reported in Ricles et al. (2002). The connection stiffness after decompression is called residual stiffness. Figure 5 illustrates the contour of equivalent plastic strain (EPEQ) for specimen PC3, at a story drift of 3.5%. This indicates that the accumulated damage is confined to the angles, as is expected for well-designed PT connections.

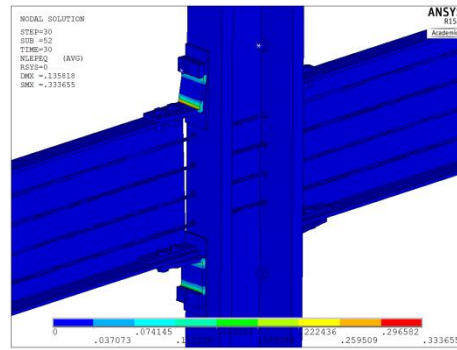


Figure 5: Equivalent plastic strain contour for specimen PC3 at 3.5% drift

The analysis of specimen PC4, which has a lower g/t than specimen PC3, exhibits greater strength, residual stiffness, and energy dissipation capacity (see Figure 4). The finite element analysis for PC4 also shows early yielding of the tensile bolts at 1.75% story drift. The von Mises stress distribution in the tensile bolt is shown in Figure 6. This result is in agreement with the reported experimental study in Ricles et al. (2002).

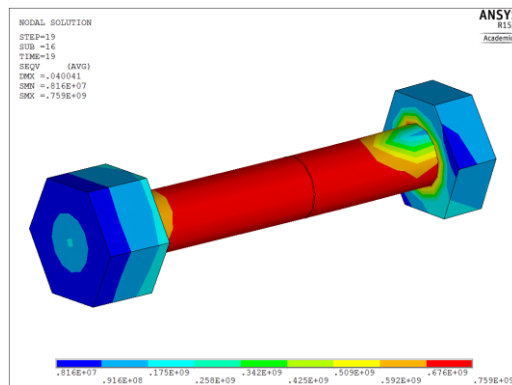


Figure 6: Early yielding of horizontal bolts in specimen PC5

By comparing the analytical response parameters with the corresponding experimental response quantities in Ricles et al. (2002), the capability of the finite element analysis to predict the cyclic behaviour of PT connections was confirmed. The analytical response was, on average, 1.08, 0.99, 1.07, 1.06, and 1.04 of the corresponding quantity reported in the test for peak relative rotation between the beam and column, maximum PT strand force, initial stiffness, the decompression moment, and the maximum connection moment, respectively. Further details of the validation study are available in Moradi & Alam (2016).

This validation of the finite element analysis however is limited to the test results for a few number of PT steel beam-column connection specimens. Further experimental tests can be performed to comprehensively validate the accuracy of the finite element predictions. Additionally, the analysis does not capture material fracture (which is particularly important for the behaviour of steel angles), fatigue behaviour of angles, dynamic and loading rate effects, and out-of-plane deformations of the connection components. Therefore, more detailed finite element models can be developed in future research to include possible effects of these factors. Based on the validation study, these factors however will not have significant effects on the lateral response of PT connections with the section sizes, material properties, and specifications in the order of those used in the reference experimental test.

5. PARAMETRIC STUDIES

Using the validated finite element model, additional analyses were performed to investigate the effects of three factors on the cyclic response. These factors are the amount of initial post-tensioning strand force, the presence of beam flange reinforcing plates, and the material properties of steel angles.

Running the model for PC1 with different initial post-tensioning strand forces (T_i) demonstrates that the connection stiffness, strength, and gap opening behaviour are affected by this factor. Figure 7 illustrates the force-displacement response curves for PC1 with different initial post-tensioning strand forces (94 kN, 117 kN, 130 kN, and 157 kN). Connections with higher T_i display lower gap opening, greater strength and stiffness, and higher energy dissipation. This result is evident in Figure 7. Note that higher values of T_i may lead to the early yielding of the PT strands and local buckling (damage) in the beam [as also observed by Garlock et al. (2005)].

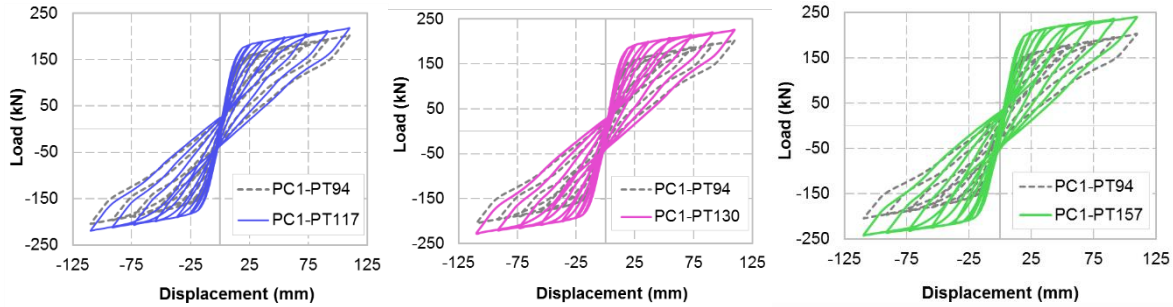


Figure 7: Effect of strand PT force on the cyclic response [adapted from Moradi & Alam (2016)]

To examine the influence of using beam flange reinforcing plates, two PT connections were analyzed: connections with and without reinforcing plates denoted as withRP and noRP, respectively. Figure 8 indicates that better self-centering is obtained for the PT connection with beam flange reinforcing plates (i.e., model withRP). In addition, connection withRP displays 10.4% and 13.4% higher moment capacity and initial stiffness, respectively.

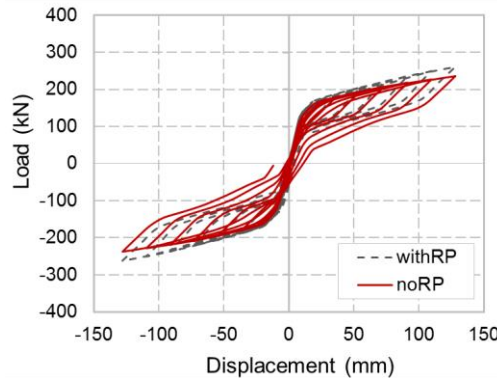


Figure 8: Effect of strand PT force on the cyclic response [adapted from Moradi & Alam (2016)]

Two different material properties were considered for the angles of the connection withRP. These models are shown in Figure 9. By comparing the hysteretic performance of the connections (wRP-AN1, wRP-AN2), it can be seen that the load capacity and energy dissipation of a PT connection are not significantly affected (less than 3%). However, early yielding of the tensile bolts was observed in the finite element analysis of the PT connection with a greater yield strength.

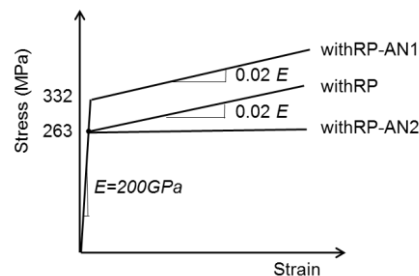


Figure 9: Material models used for angles in connections withRP, withRP-AN1, and withRP-AN2 [adapted from Moradi & Alam (2016)]

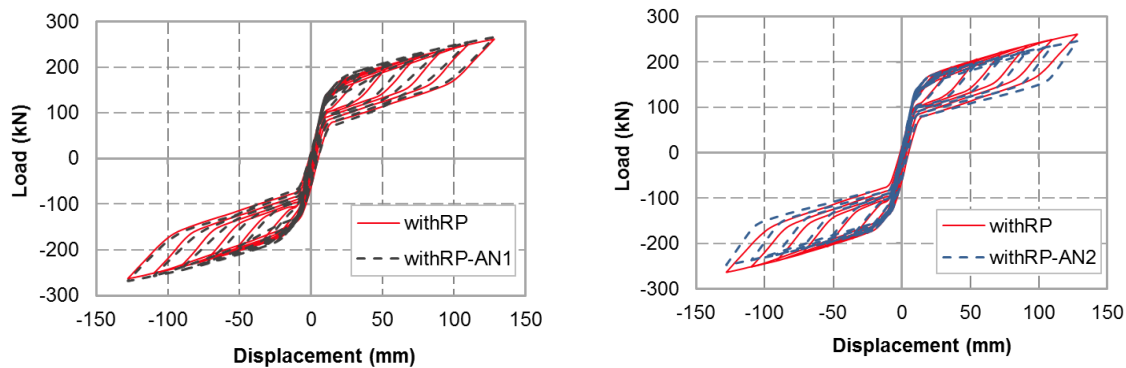


Figure 10: Effect of angle material property on the cyclic response [adapted from Moradi & Alam (2016)]

6. CONCLUSIONS

This paper presented a research effort to simulate the cyclic behaviour of post-tensioned (PT) beam-column connections. Three-dimensional finite element models of PT steel connections with top-and-seat angles were developed in ANSYS. The models were constructed using solid elements, while including material and geometric nonlinearities, contact elements, and preloading conditions for bolts and PT stands. The accuracy of the simulation was examined by comparing the analytical results with those of experiments on five full-scale interior PT connections with bolted angles. Parametric studies were also performed to investigate the influence of three different factors on the cyclic response. These factors were the amount of initial post-tensioning force in the strands, the use of beam flange reinforcing plates, and the material properties of steel angles. The following conclusions are summarized from the presented research:

- The finite element analysis predicted the cyclic performance of PT beam-column connections with adequate accuracy. The models can be therefore used for future research.
- The finite element study of PT connections can be used to capture all the possible limit states associated with the cyclic performance of PT connections, including PT strand yielding, beam local buckling, angle fracture, and the early yielding of tensile bolts.
- The initial stiffness, moment capacity, and energy dissipation of PT connections increased by using greater initial post-tensioning force in the strands.
- The use of beam flange reinforcing plates led to better self-centering behaviour, avoiding beam local buckling. Additionally, higher moment capacity and initial stiffness were observed for the connections with reinforcing plates.
- The self-centering behaviour of PT connections may be affected by the material properties of steel angles. The finite element analysis showed that the early yielding of tensile bolts may appear in case of using angles of higher strength.

The finite element modeling technique described in this paper is limited to PT steel beam-column connections with top-and-seat angles although it can be used for the simulation of steel connections with other energy dissipating mechanisms. Other limitations of the presented finite element study are that the analysis does not capture material fracture, fatigue behaviour of steel angles, dynamic and loading rate effects, and out-of-plane movement of the connection components. Future research is therefore recommended to include the potential effects of these important aspects in the finite element simulation of PT steel connections. The validation study in this paper however showed good accuracy of the finite element simulation results; therefore, the effects of these factors may not be significant for PT connections with sizes, details and specifications in the order of those used for the connections in the validation study.

ACKNOWLEDGEMENTS

The authors would like to gratefully acknowledge the financial contribution of Natural Sciences and Engineering Research Council of Canada (NSERC) through Discovery Grant. Additionally, the products and services provided by CMC Microsystems that facilitated this research, including ANSYS Multiphysics are acknowledged.

REFERENCES

- ANSYS, 2013. ANSYS Mechanical APDL, Release 15.0.
- ANSYS, 2013a. ANSYS documentation.
- Christopoulos, C. et al., 2002. Posttensioned energy dissipating connections for moment-resisting steel frames. *Journal of Structural Engineering*, 128(9), pp.1111–1120.
- Garlock, M.M., Ricles, J.M. & Sause, R., 2005. Experimental studies of full-scale posttensioned steel connections. *Journal of Structural Engineering*, 131(3), pp.438–448.
- Garlock, M.M., Sause, R. & Ricles, J.M., 2007. Behaviour and design of posttensioned steel frame systems. *Journal of Structural Engineering*, 133(3), pp.389–399.
- Hajjar, J. et al., 2013. *A synopsis of sustainable structural systems with rocking, self-centering, and articulated energy-dissipating fuses*, Boston, Massachusetts.
- Kim, H.-J. & Christopoulos, C., 2009a. Numerical models and ductile ultimate deformation response of post-tensioned self-centering moment connections. *Earthquake Engineering & Structural Dynamics*, 38(1), pp.1–21.
- Kim, H.-J. & Christopoulos, C., 2009b. Seismic design procedure and seismic response of post-tensioned self-centering steel frames. *Earthquake Engineering & Structural Dynamics*, 38(3), pp.355–376.
- Kulak, G.L., 2005. *High strength bolting for Canadian engineers*, Toronto, Ont.: Canadian Institute of Steel Construction.
- Menna, C., Auricchio, F. & Asprone, D., 2015. Applications of Shape Memory Alloys in Structural Engineering. In *Shape Memory Alloy Engineering*. Amsterdam: Elsevier, pp. 369–403.
- Moradi, S. & Alam, M.S., 2015. Feasible Application of Shape Memory Alloy Plates in Steel Beam-Column Connections. In *Structures Congress 2015*. Reston, VA: American Society of Civil Engineers, pp. 2089–2100.
- Moradi, S. & Alam, M.S., 2016. Finite-Element Simulation of Posttensioned Steel Connections with Bolted Angles under Cyclic Loading. *Journal of Structural Engineering*, 142(1), p.04015075.
- Moradi, S., Alam, M.S. & Asgarian, B., 2014. Incremental dynamic analysis of steel frames equipped with NiTi shape memory alloy braces. *The Structural Design of Tall and Special Buildings*, 23(18), pp.1406–1425.
- Moradi, S., Alam, M.S. & S. Milani, A., 2015. Cyclic Response Sensitivity of Post-tensioned Steel Connections using Sequential Fractional Factorial Design. *Journal of Constructional Steel Research*, 112, pp.155–166.
- Ozbulut, O.E., Hurlbaas, S. & Desroches, R., 2011. Seismic response control using shape memory alloys: a review. *Journal of Intelligent Material Systems and Structures*, 22(14), pp.1531–1549.
- RCSC, 2009. *Specification for Structural Joints Using High-Strength Bolts*, Chicago, IL.: Research Council on Structural Connections, American Institute of Steel Construction.

- Ricles, J.M. et al., 2002. Experimental evaluation of earthquake resistant posttensioned steel connections. *Journal of Structural Engineering*, 128(7), pp.850–859.
- Ricles, J.M. et al., 2001. Posttensioned seismic-resistant connections for steel frames. *Journal of Structural Engineering*, 127(2), pp.113–121.
- Rojas, P., Ricles, J.M. & Sause, R., 2005. Seismic performance of post-tensioned steel moment resisting frames with friction devices. *Journal of Structural Engineering*, 131(4), pp.529–540.
- Vasdravellis, G., Karavasilis, T.L. & Uy, B., 2013a. Finite element models and cyclic behaviour of self-centering steel post-tensioned connections with web hourglass pins. *Engineering Structures*, 52, pp.1–16.
- Vasdravellis, G., Karavasilis, T.L. & Uy, B., 2013b. Large-Scale experimental validation of steel posttensioned connections with web hourglass pins. *Journal of Structural Engineering*, 139(6), pp.1033–1042.
- Wolski, M., Ricles, J.M. & Sause, R., 2009. Experimental study of a self-centering beam–column connection with bottom flange friction device. *Journal of Structural Engineering*, 135(5), pp.479–488.